IGARSS 2024 - 2024 IEEE International Geoscience and Remote Sensing Symposium | 979-8-3503-6032-5/24/$31.00 ©2024 IEEE | DOI: 10.1109/IGARSS53475.2024.10640634

FLOOD IMPACT RISK MAPPING IN SETTLEMENT AREAS FROM A 3D PERSPECTIVE: A CASE STUDY OF HURRICANE MATTHEW

Jeffrey Blay, Mulham Fawakherji, Leila Hashemi-Beni
College of Science and Technology, North Carolina A&T State University, Greensboro, NC-USA
jblay@aggies.ncat.edu, mfawakherji@ncat.edu , lhashemibeni@ncat.edu

ABSTRACT

This study investigates an approach to map 3D flood map (i.e., floodwater extent and depth) using UAV high resolution imagery and LiDAR for Hurricane Matthew. We utilize a deep learning approach to map flooded areas from post event UAV images, and then employ spatial statistics to estimate the water depth of the flooded areas leveraging on the DEM. Afterward, an auxiliary dataset is combined with the generated flood depth result to map and analyze flood impact risk in settlement areas within the study area. Our result showed that settlement areas in Grifton exhibit different risk levels from a 3D flood depth perspective. This information could significantly enhance near real-time emergency response strategies, as well as future mitigation initiatives.

1. INTRODUCTION

Flooding stands as one of the most severe natural disasters that threaten human settlement areas. Flood frequencies are projected to increase globally where 48% of global land area, 46% of global assets, and 52% of the global population will be at risk of flooding by 2100 [1]. The repercussions of flooding are profound; they include the loss of life and extensive property damage. In the United States, for instance, floods caused by Hurricane Harvey in 2017 destroyed about $125 billion in property damages [2]. In the US and many other countries, the frequency of flooding and its severity have increased due to climate change effects and rapid urbanization [3]. It is projected that in areas near rivers, a 100-year flood will occur every 10-50 years [1]. Therefore, mapping flood extent and their corresponding water depth forms a pivotal aspect of developing solutions aimed at mitigating and adapting to the devastating consequences of flooding.

From the literature, numerous studies have utilized various approaches and remote sensing techniques to map flood extent and estimate water depth. [1] utilized a fully integrated model that leverages UAV sensors to map flood extent and estimate water depth [2-6]. This utilized the UAV to generate flood map extent and corresponding DEM from the UAV sensors to map and estimate the flood water extent and depth, respectively. [9] then leveraged flood map extent and lidar-generated DEM to map flood extent and estimate water depth. Also, [7] calculated flood water depth utilizing photogrammetric techniques and topographic data. All these methods leverage a similar approach and only differ in how they estimate and reconstruct the 3D water surface and the type of elevation data used.

This study contributes to the existing literature, by utilizing deep learning to map flood map extent from UAV and leveraging lidar DEM to estimate flood water depth from hurricane Matthew. The study further introduces an auxiliary dataset (built-up surface) to the estimated flood water depth for mapping flood risk in settlement areas.

2. METHODOLOGY

This study develops a 3D risk map in smaller settlement areas from a 3D perspective. The workflow is shown in Figure 1.Our study area is Grifton, a small town in Southern Pitt County in North Carolina, US. It has a population of about 2.7 thousand. Hurricane Matthew, which occurred in October 2016, caused severe flooding and damage in major cities in North Carolina. Also, small communities such as Grifton suffered severe damage. It is therefore prudent to analyze such impact in such smaller communities that are usually ignored.

2.1. Floodwater Extent Delineation

In the initial phase of our methodology, we focus on flood extent mapping, where the primary objective is to perform pixel-wise classification for the input image into two classes: 'flooded' and 'non-flooded'. In this work, we adopt a deep learning-based approach for flood mapping through semantic segmentation. Our proposed architecture is based on the pre-trained U-Net model [15], initially trained on the ImageNet dataset. UNet, as the most classic and widely used segmentation network, serves as the foundational framework for our approach. It features a typical encoding (down-sampling) and decoding (up-sampling) model, consisting of 4 up-sampling and 4 down-sampling layers each, with 2–3 stacked convolutional layers in each sampling layer. The channel counts for these layers are set at 64, 128, 256, 512, and 1024, displaying a symmetrical structure in both the encoder and decoder. The feature maps of the up-sampling and down-sampling layers are seamlessly reconnected through a concatenation function, aiding in the recovery of details lost during the max pooling process. Subsequently, the output of the segmentation step is fed into the next stage, which involves flood depth estimation.

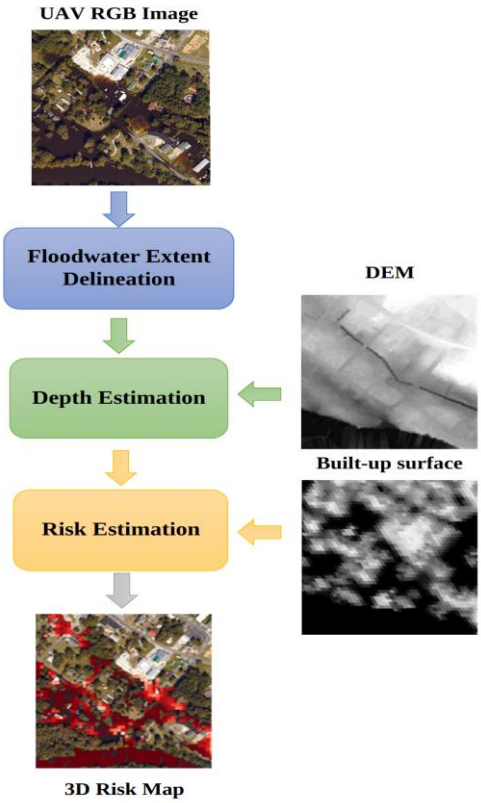

Figure 1. General workflow for our methodology

2.2. Floodwater Depth Estimation

We leverage methods employed by various studies [1], [7], [9], [10] to estimate the floodwater depth. This is a simple but comprehensive approach that only requires the flood water extent and a corresponding Digital Elevation (DEM) for estimating flood depth. It is a pixel-to-pixel calculation of deducting flood water elevation above sea mean level from the corresponding Digital Elevation Model (DEM) within the flooded domain [9].

We estimated the flood depth following these steps; (1) Clip the DEM to the shape of the flood water extent; (2) Convert the flood extent to polylines and further convert it to a raster layer; (3) Estimate the elevation values of the flood extent raster layer from the surrounding DEM pixels using spatial statistics; (4) Refine raster values using a topo slope, from the clipped DEM, (5) Utilized statistical methods to allocate flood water elevation values per cell, based on the elevation values of the nearest boundary cell of the raster polyline;(6) Calculate flood water depth by deducting the flood water elevation values from the corresponding clipped DEM:

$$D_t = F_t - E_t \qquad (1)$$

Where,

D_t is the estimated flood water depth at pixel t, F_t is the allocated flood water elevation value at pixel t, E_t is the topographic elevation value at pixel t.

3. IMPLEMENTATION AND RESULTS

The methodology was implemented in Python and spatial analyses were done using Esri GIS software. The research data includes the high-resolution UAV imagery captured by NOAA from the flooding due to Hurricane Matthew from Grifton, NC, USA (Figure 2). The data can be downloaded from the NOAA web portal.

Figure 2. Post flood UAV imagery for Grifton

3.1. Flood Extent Mapping

The proposed UNet [11] was trained through a two-step process. Initially, the encoder was initialized with weights obtained from pre-training on the ImageNet dataset. Subsequently, the entire network underwent training using Stochastic Gradient Descent (SGD) with a fixed learning rate of 1e-4 and a momentum of 0.90. The optimization aimed at minimizing the cross-entropy loss.

The training was conducted using mini batches, each comprising 16 images. To train our model, we employed the Deep Flood dataset [12], a semantic segmentation dataset derived from two flood events in North Carolina—namely, Matthew and Florence. This dataset consists of 120 images, each accompanied by a ground truth mask featuring four labels: inundated vegetation, dry vegetation, water, and others. To simplify the task, we created a binary ground truth mask i.e., 0 for non-flooded areas, and 1 for flooded areas. For the training phase, 80% of the dataset was utilized, while the remaining 20% was reserved for evaluating the model's performance.

The results indicate a high level of accuracy and performance of the proposed model in the semantic segmentation of flood areas achieving a general accuracy of 0.9697. The low general loss and high accuracy suggest that the model effectively learned to differentiate between flooded and non-flooded areas. The high IoU values further validate the model's ability to segment the regions of interest accurately. These results highlight the potential of the proposed model for flood mapping applications and underscore its

effectiveness in handling real-world flood events. The open flood water including permanent water bodies was then filtered and clipped to the area of interest to delineate the floodwater extent.

3.2. Flood Depth Estimation

Using the flood extent as an outline, we created a new DEM raster clipped to the flood extent. The flood polygon extent was then converted to polyline, and further into a raster layer. The raster polyline constitutes the boundary raster cells of the flooded extent with the same cell size (10 meters) as the DEM. We then extracted the elevation values of the boundary cells from the corresponding DEM values. The boundary cell values were further smoothened by using focal statistics based on 5 focal iterations for noise removal. For each iteration, the elevation value of a boundary cell is smoothened based on the mean of the 5 surrounding cells. Then, we calculated a topo slope from the DEM, as a condition to further filter and remove erroneous boundary cells.

We then created a cost raster from the DEM based on the condition that, areas with elevation values equal to or less than 0 be assigned 100, and all other areas be 1.This was done to prevent the estimation of elevation values over permanent water, by assigning high cost to such areas. Based on the cost raster and the boundary raster cell, the cost allocation tool [13] was utilized to estimate the elevation values within the flooded extent. Finally, the result was subtracted from the clipped DEM raster to get the flood water depth. The results were further evaluated using the RMSE. We encountered difficulties in obtaining ground truth reference water depth data from the study area. So, to overcome the challenge, we estimated the RMSE score from 10 ground truth points using a reported average water depth level in eastern North Carolina [14].

3.3. 3D Risk Analysis

We then leveraged on the estimated flood depth and built-up data to spatially map and estimate risk for the study area. The built-up surface data is spatial raster data that shows the distribution of total built-up surfaces in square meters, created by the Global Human Settlement Layer (GHSL) [10]. The pixel values of the two datasets were first normalized, and then combined to estimate risk within the study area. With this approach, areas with high pixel values in built-up and flood depth will have high risk, and vice versa:

$$R_a = FD_a + BS_a \quad (2)$$

Where, R_{at} is the estimated flood risk at cell a; FD_a is the estimated flood water depth at cell a; BS_a is the estimated built-up surface at cell a.

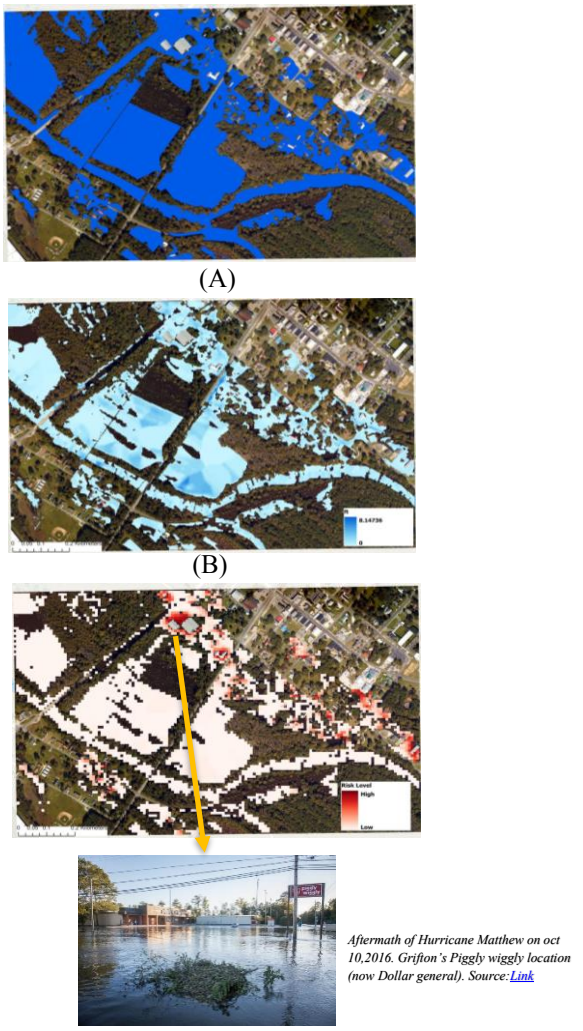

Figure 3. (A) Floodwater extent. (B) Flood depth estimation. (C) Estimated risk map.

Our results show a maximum flood depth of 8ft within the study area. From the National Hurricane Center report [13], the average water level was 2.5ft above ground level in eastern North Carolina. Using this as a reference point for accuracy, our water depth result had a 0.88 RMSE score. This suggests that on average, our estimated water depths deviate from the reference groundwater depth level by approximately 0.88 ft.

It could also be indicated that the flood areas with high flood depth are located within the non-built-up areas. However, there are areas within the built-up areas with high flood depth, especially along the central north of the main road across the study area. Also, the flood water within the built-up areas located in the northern and eastern parts of the study area shows high depth compared to the flood water within the built-up areas in the south-western part (Figure 3B).

This spatial contrast is reflected in the risk analysis (Figure 3C). The built-up areas within the north, through to the eastern part of the study area show a high risk of flood damage compared to the built-up areas within the southwestern part of the study area. This revelation could significantly influence and direct emergency response initiatives and adaptation strategies (Figure 4).

(A)

(B)

Figure 4. (A) 3D map of flood water depth (B) 3D map of flood risk level in Grifton

4. CONCLUSION

This study maps flood water extent and estimates flood depth from Hurricane Matthew in North Carolina. The study leverages on existing methods in the literature to estimate flood depth and introduces an auxiliary dataset for mapping flood risk in settlement areas from a 3D perspective. Our findings show that settlement areas within the study area show different risk levels considering the 3D water depth. Results from the flood map show an accuracy of 0.97 and the estimated flood depth deviates from the ground truth by about 0.88ft. For future studies, a more comprehensive approach with other auxiliary spatial information will significantly enhance the accuracy of the results and analysis [. Also, getting accurate reference data for evaluation could further inform and enhance the effectiveness of future studies.

5. ACKNOWLEDGMENT

This work was supported in part by NOAA award NA21OAR4590358, NASA award 80NSSC23M0051, and NSF grant 1800768.

6. REFERENCES

[1] K. J. Wienhold, D. Li, W. Li, and Z. N. Fang, "Flood Inundation and Depth Mapping Using Unmanned Aerial Vehicles Combined with High-Resolution Multispectral Imagery," *Hydrology*, vol. 10, no. 8, p. 158, Jul. 2023, doi: 10.3390/hydrology10080158.

[2] A. Salem and L. Hashemi-Beni, "Inundated vegetation mapping using sar data: A comparison of polarization configurations of uavsar l-band and sentinel c-band". Remote Sensing, 14(24), 6374, 2022.

[3] A. A.GA. Gebrehiwot. Hashemi-Beni, "A method to generate flood maps in 3D using DEM and deep learning". The International Archives of the Photogrammetry, Remote Sensing and Spatial Information Sciences, 44, 25-28, 2022.

[4] J. Yang, L. El Mendili, Y. Khayer, S. McArdle, L. Hashemi Beni, "Instance Segmentation of Lidar Data with Vision Transformer Model in Support Inundation Mapping under Forest Canopy Environment", Int. Arch. Photogramm. Remote Sens. Spatial Inf. Sci., XLVIII-1/W2-2023, 203–208, 2023.

[5] A. A.GA. Gebrehiwot. Hashemi-Beni, "3D Inundation Mapping: A Comparison Between Deep Learning Image Classification and Geomorphic Flood Index Approaches", Front. Remote Sens., Volume 3 - 2022 | https://doi.org/10.3389/frsen.2022.868104.

[6] L. Hashemi-Beni, D. Fogelman, G. Thompson, A. Gebrehiwot. "Inundation mapping using UAVs: Fixed wing vs. multirotor". Presented at the FIG e-Working Week, 2021, 21-25.

[7] A. A. Gebrehiwot and L. Hashemi-Beni, "Three-Dimensional Inundation Mapping Using UAV Image Segmentation and Digital Surface Model," *ISPRS Int. J. Geo-Inf.*, vol. 10, no. 3, p. 144, 2021.

[8] L. Hashemi-Beni and A. A. Gebrehiwot, "Flood Extent Mapping: An Integrated Method Using Deep Learning and Region Growing Using UAV Optical Data," *IEEE J. Sel. Top. Appl. Earth Obs. Remote Sens.*, vol. 14, pp. 2127–2135, 2021, doi: 10.1109/JSTARS.2021.3051873.

[9] S. Cohen *et al.*, "The Floodwater Depth Estimation Tool (FwDET v2.0) for Improved Remote Sensing Analysis of Coastal Flooding," Hydrological Hazards, preprint, Mar. 2019. doi: 10.5194/nhess-2019-78.

[10] G. Schumann *et al.*, "High-Resolution 3-D Flood Information from Radar Imagery for Flood Hazard Management," *IEEE Trans. Geosci. Remote Sens.*, vol. 45, no. 6, pp. 1715–1725, Jun. 2007, doi: 10.1109/TGRS.2006.888103.

[11] Olaf Ronneberger, Philipp Fischer, and Thomas Brox, "U-net: Convolutional networks for biomedical image segmentation," in Medical Image Computing and Computer-Assisted Intervention – MICCAI 2015.

[12] M. Fawakherji, M. Anokye, J. Blay, and L. Hashemi-Beni, "Multichannel Deep Learning-based Architecture for Flood Detection and Mapping," *2023 AGU Conf.*, 2023.

[13] ESRI, "Cost Allocation, ArcGIS Pro 2.0", Accessed: Dec. 28, 2023.[Online].Available:https://pro.arcgis.com/en/pro-app/latest/tool-reference/spatial-analyst/cost-allocation.htm

[14] R. Berg, "Hurricane Matthew," 2017, [Online]. Available: https://www.nhc.noaa.gov/data/tcr/AL142016_Matthew.pdf

[15] M. Pesaresi and Politis P, "GHS-BUILT-S R2023A - GHS built-up surface grid, derived from Sentinel2 composite and Landsat, multitemporal (1975-2030).," *Eur. Comm. Jt. Res. Cent. JRC*,2023.